Optical detection of Sm^{2+} nuclear quadrupole resonances in SrFCl and BaFCl

Optical detection of Sm^{2+} nuclear quadrupole resonances in SrFCl and BaFCl

R Jaaniso† and H Bill

Department of Physical Chemistry, University of Geneva, 30 quai Ernest-Ansermet, CH-1211 Geneva 4, Switzerland

Abstract. We report the first observation of nuclear quadrupole resonances in Sm^{2+}, detected optically for both naturally occurring isotopes with nuclear spin (Sm^{147} and Sm^{149}) in SrFCl and BaFCl crystals. Quadrupole coupling constants P are determined in the $^7F_0$ electronic ground state and estimates are given for the ratios of shielding parameters $(1 - \gamma_\infty)/(1 - \sigma_2)$. Comparison of the two crystals demonstrates the sensitivity of quadrupolar coupling to Sm^{2+}–ligand interactions. Anomalously small splittings in BaFCl ($|P| < 0.05$ MHz) are ascribed to the mutual cancelling of two electric field gradient components (4f shell and direct crystal field terms).

The detection of hyperfine or nuclear quadrupole resonances (NQRs) based on the pumping of the electronic ground state sublevels with narrow-band tunable lasers has been successfully applied to study trivalent rare earth ions in solids [1]. In particular, NQR in Eu^{3+}, which is isoelectronic to Sm^{2+}, has been observed by optical methods [2, 3]. Optical detection has been noted to be especially advantageous under those circumstances where nuclear magnetic moments are strongly shielded by the environment. The latter point was first analysed by Elliott in a theoretical paper [4] dealing with magnetic and quadrupolar interactions in Eu^{3+}. For Sm^{2+} the situation is probably even worse for conventional NMR, as the nuclear gyromagnetic ratios themselves are three–six times smaller than for Eu^{3+}. In the present article, ODNQR measurements are described for the first time for Sm^{2+}.

The study is based on the finding that the ground state sublevels of Sm^{2+} in MeFX type crystals can be optically pumped via degenerate $^5D_1(E)$ excited states [5]. Sm^{2+} enters substitutionally into these crystals by occupying the cationic site with C_{4v} symmetry. Structural data [6] as well as crystal field parameters determined from optical spectra [7, 8] are available for BaFCl and SrFCl hosts, which gives the possibility of comparing the shielding effects in crystals of the same structure ($P4/nmm$, D_{4h} point symmetry) and close composition. Single-crystal species with a nominal Sm doping level of 0.02–0.3 at.% were grown as described in [9].

Optical pumping of the ground state sublevels was performed at the centre of the $^5D_1(E)$–$^7F_0(A_1)$ transition (near 630 nm) using a single-frequency dye laser (CR 699-21, linewidth < 2 MHz). Irradiation on this transition (typically 1 s at 0.1 mW cm^{-2}) produced a narrow and stable hole in the inhomogeneously broadened spectrum. Figure 1 shows two holes, burned successively at two different frequencies, and detected in the fluorescence excitation spectrum. The holes, which showed characteristic antiholes on both sides, could

† Permanent address: Institute of Physics, Estonian Academy of Sciences, Riia 142, EE-2400 Tartu, Estonia.

be burned at temperatures $T \leqslant 22$ K. Below $T = 8$ K, the hole decay time was determined to be longer than 1 h. Maximum relative hole depth (23%) was close to the total natural abundance of stable Sm isotopes with nuclear spin (15.0% for Sm^{147} and 13.8% for Sm^{149}, $I = \frac{7}{2}$ for both isotopes [10]). As will be shown below, all the ground state quadrupole splittings are smaller than 2 MHz. The appearance of antiholes at 20–40 MHz distance is therefore related to the hyperfine splittings in the excited E state (figure 1, inset). Further details concerning optical hole burning will be given elsewhere. We simply add here that the hole burning (i.e. optical pumping) yield was estimated to be relatively high, greater than 10%.
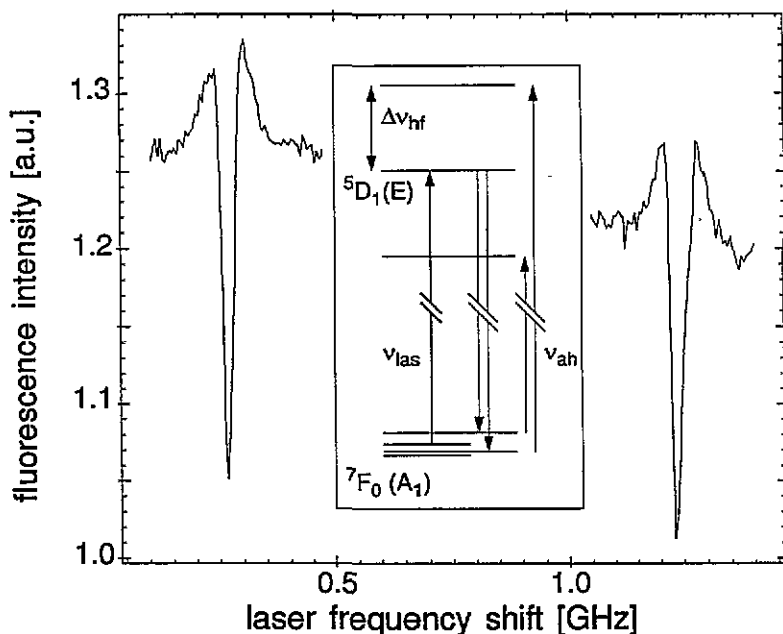

Figure 1. Spectral holes in the fluorescence excitation spectrum of Sm^{2+}:SrFCl. Inset: simplified scheme of optical pumping. Only three of eight excited state hyperfine levels and only the pumping from an $I_z = \pm\frac{5}{2}$ ground state level are shown (ν_{las} is the laser frequency). Increased population in the ground state $\pm\frac{7}{2}$ and $\pm\frac{3}{2}$ levels leads to the appearance of antiholes at the probe frequencies $\nu_{ah} \simeq (\nu_{las} \pm \Delta\nu_{hf})$.

Ground state NQRs were detected by RF-induced hole filling [11]. At the fixed laser frequency the intensity of non-resonant fluorescence ($\lambda > 690$ nm) was monitored during the RF scan. When the resonance occurs between ground state sublevels, then the Sm^{2+} ions pumped to another sublevel during initial optical irradiation (hole burning) will be partly returned to the original optical frequency. As a result, the absorbance at the laser frequency, and the fluorescence intensity, will be increased. An RF field was provided by a computer controlled synthesizer, 200 W amplifier, and three-turn coil around the sample. The following measurement method was used: between two signal count periods (A and B) of equal length an RF pulse (~ 100 W) was applied, and the difference spectrum (A − B) was recorded. Typical RF pulse lengths were 0.1–0.3 s at a duty cycle of 20%. Before the synthesizer output frequency was turned to a new value, the light intensity on the sample

was increased for a short time (from 0.01 to 5 mW cm^{-2} for 0.2 s) in order to keep the difference in sublevel populations at a maximum level. In all measurements the samples were held in liquid He at $T = 2$ K.

The sublevel energies in a $^7F_0$ state should be determined by similar factors as for the isoelectronic Eu^{3+} [4, 12]. For a C$_{4v}$ symmetry site,

$$E = P[I_z^2 - I(I + 1)/3] \qquad (1)$$

$$P = P_{latt} + P_{4f}^{(2)} + P_{pq} \qquad (2)$$

where P_{latt} is the direct crystal field gradient term, $P_{4f}^{(2)}$ is the second-order contribution from 4f electrons (arising from $J \neq 0$ states mixed to the ground state by the crystal field), and P_{pq} is the second order hyperfine (pseudo-quadrupole) term.

Experimental spectra for Sm^{2+}: SrFCl are shown in figure 2. One observed two sets of lines (corresponding to two isotopes) with the frequencies of one set in the ratio of 1:2:3. The latter ratios are fulfilled exactly within experimental error limits, which shows that the spectra are characteristic for an $I = \frac{7}{2}$ spin under axial symmetry, thus confirming our initial assignment of the hole burning mechanism. Figure 3 presents corresponding spectra in the BaFCl host, where the resonances were found at markedly lower frequencies. The lines are broader and only two Sm^{147} transitions ($\frac{3}{2} \leftrightarrow \frac{5}{2}$ and $\frac{5}{2} \leftrightarrow \frac{7}{2}$) are clearly resolved. The absolute values of the coupling constants, determined in SrFCl and BaFCl at $T = 2$ K, are given in table 1.

The lines could be fitted with Gaussian or Voigt profiles. This difference was not investigated in detail, but it probably arose due to slightly different degrees of saturation. To avoid significant distortions, the RF pulse areas were adjusted so that the difference signal was below its maximum (fully saturated) value. In addition, the coincidence of the resonance peak positions at two different directions of RF sweep was checked. The linewidths are almost equal for all the transitions of one isotope in a given host: 1.7–1.9 kHz for Sm^{149}: SrFCl, 5–7 kHz for Sm^{147}: SrFCl, and 25 kHz for Sm^{147}: BaFCl. As the ratio of the linewidths for two isotopes in SrFCl is approximately equal to the ratio of the corresponding quadrupole moments, one can ascribe the broadening to the (strain induced) random field gradients. The violation of 1:2:3 ratio for the linewidths of one isotope can then be explained by the influence of low-symmetry field gradients, as their contributions to the linewidth, if taken in the order of increasing I_z, are gradually decreasing. Regarding the relatively strong broadening in BaFCl, we note that the inhomogeneous widths of optical transitions were also bigger in this host. In addition, for perturbing uniaxial fields the ratio between 4f and lattice contributions to P may be different from that for the C$_{4v}$ main field, and thereby, the cancelling between these two contributions (which actually leads to small resonant frequencies in BaFCl, see below), may not take place for the linewidths.

Table 1. Quadrupole coupling constants $|P|$ (kHz).

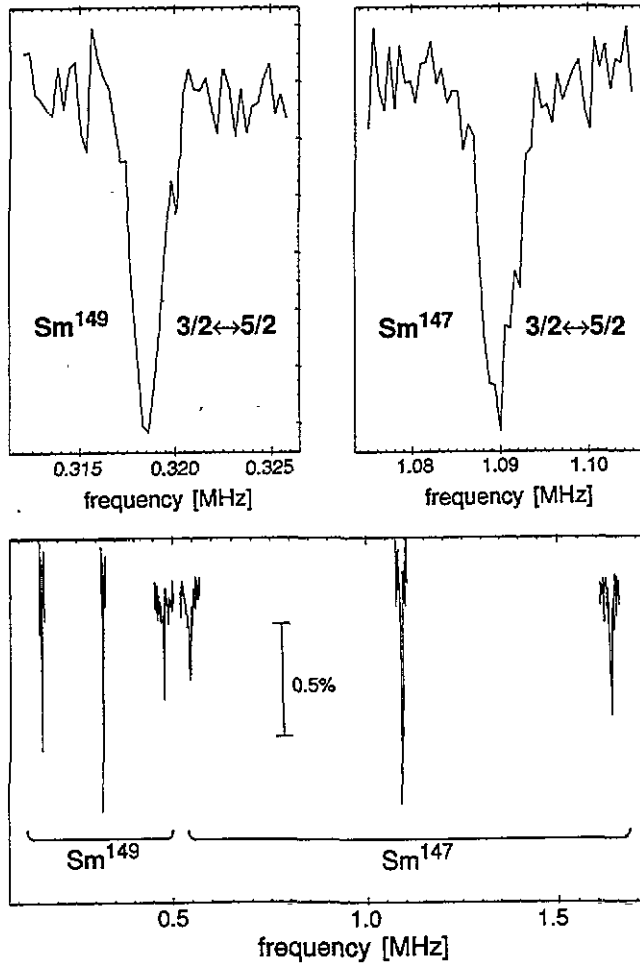| Host	Isotope	
	Sm^{149}	Sm^{147}
SrFCl	79.63(3)	272.48(6)
BaFCl	—	41.5(2)

Figure 2. ODNQR in the $^7F_0$ ground state of Sm^{2+}:SrFCl. $T = 2$ K, nominal Sm concentration = 0.02%.

In order to clarify the dependence of the field gradient on the host crystal, a detailed inspection of different contributions to P should be undertaken. The magnetic P_{pq} term can be shown to be negligible in a first approximation (analogously to Eu^{3+} [4, 13]). Substituting the values of Sm nuclear magnetic moments [10] and the required spectral data [7, 8] into the appropriate formula in [13], one obtains that $|P_{pq}| < 1$ kHz for all cases. For example, $P_{pq}(Sm^{147}) = 0.39$ kHz and $P_{pq}(Sm^{149}) = 0.27$ kHz in SrFCl. The main terms in (2) can be written as [12, 14]

$$P_{4f}^{(2)} = [6e^2 Q B_0^2 \langle r^{-3}\rangle_{4f}(1 - R_Q)/I(2I - 1)]M_{02}/\Delta_{02} \tag{3}$$

$$P_{latt} = -3Q(B_0^2 - B_{0c}^2)(1 - \gamma_\infty)/I(2I - 1)\langle r^2\rangle_{4f}(1 - \sigma_2) \tag{4}$$

where M_{02} is the squared module of the reduced matrix element $\langle ^7F_2||\alpha||^7F_0\rangle$ ($= 0.231$ [4]), and Δ_{20} is the difference between the energies of corresponding levels: $\Delta_{02}(SrFCl) = 834$ cm^{-1} [8] and $\Delta_{02}(BaFCl) = 820$ cm^{-1} [7]. The crystal field parameters B_0^2, determined from optical spectra, are equal to 58 ± 4 cm^{-1} and -93 cm^{-1}, respectively [7, 8]. B_{0c}^2 is the
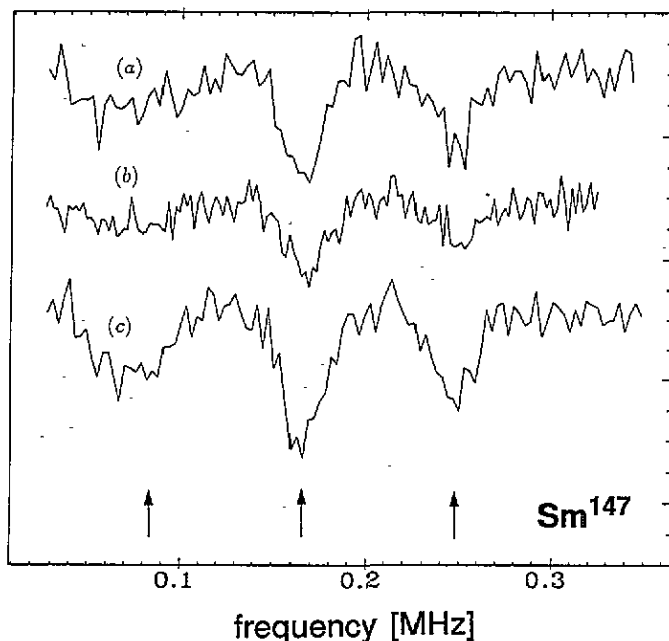
Figure 3. Sm^{2+} ODNQR in the BaFCl host at $T = 2$ K. Sm concentration $= 0.3\%$ (a, b) or 0.1% (c). Spectrum (b) was recorded at a two times smaller RF power than spectrum (a).

contact interaction part of the quadrupolar crystal field parameter, arising from 4f and ligand wave functions overlap, covalency, and charge interpenetration [14]. For free ion radial integrals we will use the values calculated by Freeman and Desclaux [15]: $\langle r^2 \rangle_{4f} = 0.33$ Å^2, $\langle r^{-3} \rangle_{4f} = 42.5$ Å^{-3}. The values of quadrupole moments, $Q(\text{Sm}^{147}) = -0.259(26)b$ and $Q(\text{Sm}^{149}) = 0.075(8)b$, are taken from [10].

γ_∞ is the lattice Sternheimer factor describing the enhancement of crystal field at the nucleus due to the polarization of closed shells, R_Q describes the screening of the field gradient set up by the partly filled 4f shell (atomic Sternheimer factor), and σ_2 is the shielding factor for the crystal field at the position of 4f electrons. Shielding factors for the Sm^{2+} free ion have been calculated by Gupta and Sen [16]: $R_Q = 0.124$, $\gamma_\infty = -73$, $\sigma_2 = 0.58$. The value of $(1 - R_Q)$ can be assumed to be relatively precise, as all the reported values for rare earths are situated in the range of $0.7 < (1 - R_Q) < 1.0$ (moreover, the coincidence of different results for a given atom or ion is better than $\pm 5\%$) [16–18]. The values of γ_∞, calculated for free ions, lie near -70 for the whole lanthanide series, and σ_2, as a rule, is between 0.5 and 0.7 [16, 17, 19, 20].

On the basis of the data given above one can evaluate the theoretical values of the 4f electron term (3), which, when subtracted from the experimental coupling constants P, yield the values for P_{latt}. The results for Sm^{147} are collected into table 2. As the sign of P was not determined from the experiment, two possibilities are shown.

It has been the usual practice to calculate the ratio $\alpha_{\text{sh}} = (1 - \gamma_\infty)/(1 - \sigma_2)$ from the expression (4) (by assuming implicitly that B_0^2 describes adequately the electrostatic field at the position of 4f electrons). The values of α_{sh}, determined by this procedure for 4f trivalent ions and summarized in [16], are all between 130 and 300. Newman and Price [14], by including the crystal field contact terms on the basis of a superposition model analysis, have

Table 2. 4f and lattice contributions to P (for Sm^{147}), and the values of α_{sh}.

Host	$P_{4f}^{(2)}$ (kHz)	sign of P	P_{latt} (kHz)	$(1 - \gamma_\infty)/(1 - \sigma_2)$
SrFCl	−356	+	628	320
		−	84	40
BaFCl	581	+	−539	170
		−	−623	200
Theoretical value for Sm^{2+} free ion [16]				180

found that the value of α_{sh} should actually be 670 for Gd^{3+}. The difference from the free ion theoretical value was ascribed to the greater 4f shielding ($\sigma_2 = 0.9$ instead of $\sigma_2 = 0.6$). Whatever the reason for the latter discrepancy, it is evident that for Sm^{2+}: SrFCl only the case $P > 0$ is consistent with previously reported data on rare earth systems. Also, if we exclude the case $P(SrFCl) < 0$, then the values of α_{sh}, given in table 2, are not so far from the theoretical one.

It further follows from table 2 that the anomalously small quadrupolar coupling in BaFCl results from the mutual cancelling of two field gradient components. The sign of P cannot be determined in this case. Nevertheless, the mean value of α_{sh} can be given with relatively high precision: $\alpha_{sh} = 185 \pm 35$ (the uncertainties of Q and B_0^2 will not be transferred into the value of α_{sh} at $P_{latt} \simeq P_{4f}^{(2)}$). For the SrFCl host the following final value can be given: $\alpha_{sh} = 320 \pm 50$. Note that a quite similar material dependence has been found for Tm^{3+} in stoichiometric compounds: $\alpha_{sh} = 250$ in Tm ethyl sulphate and $\alpha_{sh} = 130$ in Tm_2O_3 [21].

Alternatively, by adopting the assumption of [14] (the effect of 4f contact terms should be taken into the account in the first order; shielding factors do not depend on the environment), it follows from table 2 that the pure electrostatic field ($B_0^2 - B_{0c}^2$) is nearly equal by its absolute value but has opposite sign in the two studied compounds. Consequently, under this assumption the contact parts of the quadrupolar crystal field parameters should fulfill the relation $B_{0c}^2(BaFCl) + B_{0c}^2(SrFCl) \simeq -35$ cm^{-1}, which means that at least $\sim 25\%$ of the B_0^2 value is due to unshielded 4f–ligand interactions. This relative size of B_{0c}^2 is indeed rather common in different types of crystal [22]. For Sm^{2+} in SrFCl and BaFCl the crystal field has been parametrized within the frame of the angular overlap model [7, 8], but the role of contact-type interactions has not been separated. Still, these interactions are probably not negligible, as the ratios B_0^4/B_4^4 and B_0^6/B_4^6 were shown to be markedly different from corresponding electrostatic model ratios. It is also worth noting here that the ligand contributions to the B_0^2 parameter tend to be extremely sensitive to small angular changes in the present crystals [23].

Regarding the possible host dependence of the (anti)shielding factors, the necessity of considering the 5p,6s–ligand overlap has been suggested for both σ_2 and γ_∞ [16, 19, 24]. At the interpretation of experimental data it has been most frequently assumed that only the shielding of the 4f shell is sensitive to the chemical bonding (see, e.g., [12, 21]). Model calculations of the Sternheimer antiscreening in the Pr^{3+}–Cl^- system showed that the charge redistribution in the overlap region leads to the reduction of the γ_∞ value (by 20–40%), but only a weak radial dependence of γ_∞ was found at typical ionic distances [24]. A crude way to estimate the sensitivity of shielding factors to the expansion of the wave function is to compare the different results obtained with the same calculation method but using different free ion wave functions. For the most studied ions, Tm^{3+} and Pr^{3+} [16, 17, 19, 20, 25], we actually found that the results differ by $\sim 10\%$ for σ_2, and by $\sim 20\%$ for γ_∞ ($\langle r^2 \rangle$ variations being also about 20%). In the light of these data sizeable effects due to the (anti)shielding

factors cannot be excluded. However, in order to give any estimates for these factors in the studied compounds, detail theoretical modelling is needed, especially with respect to the angular dependence.

To summarize, we conclude that, although no final mechanism can be indicated at the present stage, the host dependence of quadrupolar coupling is essentially determined by Sm^{2+}–ligand interactions. In the frame of a simple electrostatic model (electric field gradient at the nucleus is proportional to B_0^2 and shielded charges are completely external with respect to the Sm^{2+} ion), the NQR frequencies of Sm^{2+} should be 1.6 times bigger in BaFCl. In reality, they are six times smaller in this host. This discrepancy is demonstrated to be either due to a $\sim$ 50% difference in the shielding factors (different 5p–ligand overlap in the two crystals), or due to $\geqslant$ 25% contribution from 4f–ligand contact interactions into B_0^2. The given estimates (or limits) for α_{sh} and B_{0c}^2 may serve as the starting values for further detailed crystal field calculations on the studied systems.

The ratio of quadrupole moments can also be estimated for the two Sm isotopes. After substraction of small pseudo-quadrupolar corrections from the data given in table 1 for Sm^{2+}:SrFCl, one obtains $Q(147)/Q(149) = -3.429(2)$. This can be compared to the values determined for neutral Sm from atomic beam magnetic resonance data, $-3.4601(3)$ [26], and for Sm^{3+}:LaCl$_3$ from ENDOR spectra, $-3.392(14)$ [27]. We note that our value may include an additional error, because P_{pq} was calculated using the free ion parameters. Taking into account that deviations of up to 10% have been determined for the magnetic moment matrix elements in the BaFCl crystal [28], we estimated the uncertainty of the above given quadrupole moment ratio to be $\pm$1.2%. An improvement of the preciseness would be of interest (for example, by measuring the $^5D_0$ state NQR [29]), especially because no external magnetic field corrections are needed for ODNQR data. Using the exact quadrupole moment ratio it is also possible to fill the space in table 1: $|P(\mathrm{Sm}^{149}:\mathrm{BaFCl})| = 12$ kHz.

To conclude, we note in addition to what was mentioned in the introductory paragraph that the possibility of quadrupolar sublevel pumping in Sm^{2+}:MeFX-type crystals may be useful for optical hole burning applications, especially in view of the high pumping efficiency and slow relaxation between closely spaced sublevels.

References

[1] Macfarlane R M and Shelby R M 1987 *Spectroscopy of Solids Containing Rare Earth Ions (Modern Problems in Condensed Matter Sciences 21)* ed A A Kaplyanskii and R M Macfarlane (Amsterdam: North-Holland) pp 51–184
[2] Erickson L E and Sharma K K 1981 *Phys. Rev.* B **24** 3697
[3] Shelby R M and Macfarlane R M 1981 *Phys. Rev. Lett.* **47** 1172
[4] Elliott R J 1957 *Proc. Phys. Soc.* B **70** 119
[5] Jaaniso R, Hagemann H and Bill H 1992 *Spectral Hole Burning and Luminescence Line Narrowing: Science and Applications (OSA Tech. Digest Ser. 22)* (Washington, DC: Optical Society of America) pp 79–82
[6] Sauvage M 1974 *Acta Crystallogr.* B **30** 2786
[7] Gâcon J C, Grenet G, Souillat J C and Kibler M 1978 *J. Chem. Phys.* **69** 868
[8] Grenet G, Kibler M, Gros A, Souillat J C and Gâcon J C 1980 *Phys. Rev.* B **22** 5052
[9] Nicollin D and Bill H 1978 *J. Phys. C: Solid State Phys.* **11** 4803
[10] Raghavan P 1989 *At. Data Nucl. Data Tables* **42** 189
[11] Erickson L E 1977 *Opt. Commun.* **21** 147
[12] Blok J and Shirley D A 1966 *Phys. Rev.* **143** 278
[13] Silversmith A J, Radlinski A P and Manson N B 1986 *Phys. Rev.* B **34** 7554
[14] Newman D J and Price D C 1975 *J. Phys. C: Solid State Phys.* **8** 2985

[15] Freeman A J and Desclaux J P 1979 *J. Magn. Magn. Mater.* **12** 11
[16] Gupta R P and Sen S K 1973 *Phys. Rev.* A **7** 850
[17] Sternheimer R M 1966 *Phys. Rev.* **146** 140
[18] Childs W J and Cheng K T 1984 *Phys. Rev.* A **30** 677
[19] Sternheimer R M, Blume M and Peierls R F 1968 *Phys. Rev.* **173** 376
[20] Erdös P and Kang J H 1972 *Phys. Rev.* B **6** 3393
[21] Barnes R G, Mössbauer R L, Kankeleit E and Poindexter J M 1964 *Phys. Rev.* **136** A175
[22] Newman D J and Ng B 1989 *Rep. Prog. Phys.* **52** 699
[23] Nicollin D and Bill H 1978 *Solid State Commun.* **20** 135
[24] Ahmad S and Newman D J 1978 *Aust. J. Phys.* **31** 421
[25] Gupta R P, Rao B K and Sen S K 1971 *Phys. Rev.* A **3** 545
[26] Woodgate G K 1966 *Proc. R. Soc.* A **293** 117
[27] Chan I Y and Hutchison C A Jr 1972 *Phys. Rev.* B **5** 3387
[28] Macfarlane R M, Shelby R M and Winnacker A 1986 *Phys. Rev.* **33** 4207
[29] Silversmith A J and Manson N B 1986 *Phys. Rev.* B **34** 4854